SPARSITY WINNING TWICE: BETTER ROBUST GENERALIZATION FROM MORE EFFICIENT TRAINING

Anonymous authors
Paper under double-blind review

ABSTRACT

Recent studies demonstrate the deep networks, even robustified by the state-of-the-art adversarial training (AT), still suffer from large robust generalization gaps, in addition to the much more expensive training costs than standard training. In this paper, we investigate this intriguing problem from a new perspective, i.e., *injecting appropriate forms of sparsity* during adversarial training. We introduce two alternatives for sparse adversarial training: (i) *static sparsity*, by leveraging recent results from the lottery ticket hypothesis to identify critical sparse subnetworks arising from the early training; (ii) *dynamic sparsity*, by allowing the sparse subnetwork to adaptively adjust its connectivity pattern (while sticking to the same sparsity ratio) throughout training. We find both static and dynamic sparse methods to yield win-win: substantially shrinking the robust generalization gap and alleviating the robust overfitting, meanwhile significantly saving training and inference FLOPs. Extensive experiments validate our proposals with multiple network architectures on diverse datasets, including CIFAR-10/100 and Tiny-ImageNet. For example, our methods reduce robust generalization gap and overfitting by 34.44% and 4.02%, with comparable robust/standard accuracy boosts and 87.83%/87.82% training/inference FLOPs savings on CIFAR-100 with ResNet-18. Besides, our approaches can be organically combined with existing regularizers, establishing new state-of-the-art results in AT. All codes are included.

1 INTRODUCTION

Deep neural networks (DNNs) are notoriously vulnerable to maliciously crafted adversarial attacks. To conquer this fragility, numerous adversarial defense mechanisms are proposed to establish robust neural networks (Schmidt et al., 2018; Sun et al., 2019; Nakkiran, 2019; Stutz et al., 2019; Raghunathan et al., 2019; Hu et al., 2019; Chen et al., 2020d; 2021c; Jiang et al., 2020). Among them, *adversarial training* (AT) based methods (Madry et al., 2017; Zhang et al., 2019) have maintained the state-of-the-art robustness. However, the AT training process usually comes with order-of-magnitude higher computational costs than standard training, since multiple attack iterations are needed to construct strong adversarial examples (Madry et al., 2018b). Moreover, AT was recently revealed to incur severe robust generalization gaps (Rice et al., 2020), between its training and testing accuracies, as shown in Figure 1; and to require significantly more training samples (Schmidt et al., 2018) to generalize robustly.

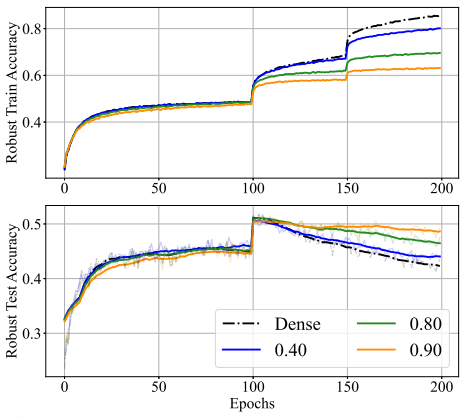

Figure 1: Robust train / test accuracy (*Top* / *Bottom*) on CIFAR-10 with ResNet-18 across various sparsity levels from 0% (Dense) to 90%. The dash-dot and solid lines represent the vanilla PGD-AT dense baseline and our sparse proposals, respectively. As the sparsity increases, the robust generalization gap between training and testing accuracy is substantially narrowed.

In response to those challenges, Schmidt et al. (2018); Lee et al. (2020); Song et al. (2019) investigate the possibility of improving generalization by leveraging advanced data augmentation techniques, which further amplifies the training cost of AT. Recent studies (Rice et al., 2020; Chen et al., 2021c) found

that early stopping, or several smoothness/flatness-aware regularizations (Chen et al., 2021c; Stutz et al., 2021; Singla et al., 2021), can bring effective mitigation.

In this paper, a new perspective has been explored to tackle the above challenges by *enforcing appropriate sparsity patterns* during AT. The connection between robust generalization and sparsity is mainly inspired by two facts. On one hand, sparsity can effectively regularize the learning of over-parameterized neural networks, hence potentially benefiting both standard and robust generalization (Balda et al., 2019). As demonstrated in Figure 1, with the increase of sparsity levels, the robust generalization gap is indeed substantially shrunk while the robust overfitting is alleviated. On the other hand, the key design philosophy that facilitates this consideration is the lottery ticket hypothesis (LTH) (Frankle & Carbin, 2019). The LTH advocates the existence of highly sparse and separately trainable subnetworks (a.k.a. winning tickets), which can be trained from the original initialization to match or even surpass the corresponding dense networks' expressiveness. These facts point out a promising direction that utilizing proper sparsity is capable of boosting robust generalization while maintaining competitive standard and robust accuracy.

Although sparsity is beneficial, the current methods (Frankle & Carbin, 2019; Frankle et al., 2020; Renda et al., 2020) often empirically locate sparse critical subnetworks by Iterative Magnitude Pruning (IMP). It demands excessive computational cost even for standard training due to the iterative train-prune-retrain process. Recently, You et al. (2020) demonstrated that these intriguing subnetworks can be identified at the very early training stage using one-shot pruning, which they term as *Early Bird* (EB) tickets. We show the phenomenon also exists in the adversarial training scheme. More importantly, we take one leap further to reveal that even in adversarial training, EB tickets can still be drawn from a cheap standard training stage, while still achieving solid robustness. In other words, *the Early Bird is also a Robust Bird* that yields an attractive win-win of efficiency and robustness - we name this finding as *Robust Bird* (RB) tickets.

Furthermore, we investigate the role of sparsity in a scene where the sparse connections of subnetworks are on the fly. Specifically, we initialize a subnetwork with random sparse connectivity and then optimize its weights and sparse typologies simultaneously, while sticking to the fixed small parameter budget. This training pipeline, called as *Flying Bird* (FB), is motivated by the latest sparse training approaches (Evci et al., 2020b; Liu et al., 2021b) to further reduce robust generalization gap in AT, while ensuring the low training costs. Moreover, an enhanced algorithm, i.e., *Flying Bird+*, is proposed to dynamically adjust the network capacity (or sparsity) to pursue superior robust generalization and performance, at minor prices of training efficiency.

Our innovative contributions can be summarized as follows:

- We perform a thorough investigation to reveal that introducing appropriate sparsity into AT is an appealing win-win, specially: (1) substantially alleviating the robust generalization gap; (2) maintaining comparable or even better standard/robust accuracies; and (3) enhancing the AT efficiency by training only compact subnetworks.
- We explore two alternatives for sparse adversarial training: (i) the *Robust Bird* (RB) training that leverages static sparsity, by mining the critical sparse subnetwork at the early training stage, and using only the cheapest standard training; (ii) the *Flying Bird* (FB) training that allows for dynamic sparsity, which jointly optimizes both network weights and their sparse connectivity during AT, while sticking to the same sparsity level. We also discuss a FB variant called *Flying Bird+* that adaptively adjusts the sparsity level on demand during AT.
- Extensive experiments are conducted on CIFAR-10, CIFAR-100, and Tiny-ImageNet with diverse network architectures. Specifically, our proposals obtain $80.16\% \sim 87.83\%$ training FLOPs and $80.16\% \sim 87.83\%$ inference FLOPs savings, shrink robust generalization from $28.00\% \sim 63.18\%$ to $4.43\% \sim 34.44\%$, and boost the robust accuracy by up to 0.60% and the standard accuracy by up to 0.90%, across multiple datasets and architectures. Meanwhile, combining our sparse adversarial training frameworks with existing regularizations establishes the new state-of-the-art results.

2 Related Work

Adversarial training and robust generalization/overfitting. Deep neural networks present vulnerability to imperceivable adversarial perturbations. To deal with this drawback, numerous defense

approaches have been proposed (Goodfellow et al., 2015; Kurakin et al., 2016; Madry et al., 2018a). Although many methods (Liao et al., 2018; Guo et al., 2018a; Xu et al., 2017; Dziugaite et al., 2016; Dhillon et al., 2018a; Xie et al., 2018; Jiang et al., 2020) were later found to result from obfuscated gradients (Athalye et al., 2018), adversarial training (AT) (Madry et al., 2018a), together with some of its variants (Zhang et al., 2019; Mosbach et al., 2018; Dong et al., 2018), remains as one of the most effective yet costly approaches.

A pitfall of AT, i.e., the poor robust generalization, was howevr noticed recently. Schmidt et al. (2018) showed that AT intrinsically demands a larger sample complexity to identify well-generalizable robust solutions. Therefore, data augmentation (Lee et al., 2020; Song et al., 2019) is an effective remedy. Stutz et al. (2021); Singla et al. (2021) related robust generalization gap to curvature/flatness of loss landscapes. They introduced weight perturbing approaches and smooth activation functions to reshape the loss geometry and boost robust generalization ability. Meanwhile, the robust overfitting (Rice et al., 2020) in AT usually happens with or as a results of inferior generalization. Previous studies (Rice et al., 2020; Chen et al., 2021c) demonstrated that conventional regularization-based methods (e.g., weight decay and simple data augmentation) can not alleviate robust overfitting. Then, numerous advanced algorithms (Zhou et al., 2021; Bunk et al., 2021; Chen et al., 2021a; Dong et al., 2021b;a; Zi et al., 2021; Tack et al., 2021; Zhang et al., 2021a) arose in the last half year to tackle the overfitting, using data manipulation, smoothened training, and else. Those methods work orthogonally to our proposal as evidenced in Section 4.

Another group of related literature lies in the filed of sparse robust networks (Guo et al., 2018b). These works either treat model compression as a defense mechanism (Wang et al., 2018; Gao et al., 2017; Dhillon et al., 2018b) or pursue robust and efficient sub-models that can be deployed in resource-limited platforms (Gui et al., 2019; Ye et al., 2019; Sehwag et al., 2019). Compared to those inference-focused methods, our goal is fundamentally different: injecting sparsity during training to reduce the robust generalization gap while improving training efficiency.

Static pruning and dynamic sparse training. Pruning (LeCun et al., 1990; Han et al., 2015a) serves as a powerful technique to eliminate the weight redundancy in over-parameterized DNNs, which aims to obtain storage and computational savings with almost undamaged performance. It can roughly divided into two categories based on how to generate sparse patterns: (i) *static pruning*. It removes parameters (Han et al., 2015a; LeCun et al., 1990; Han et al., 2015b) or sub-structures (Liu et al., 2017; Zhou et al., 2016; He et al., 2017) based on optimized importance scores (Zhang et al., 2018; He et al., 2017) or some heuristics like weight magnitude (Han et al., 2015a), gradient (Molchanov et al., 2019), hessian (LeCun et al., 1990) statistics. The discarded elements usually will not participate in the next round of training or pruning. Static pruning can be flexibly applied prior to training, such as SNIP (Lee et al., 2019), GraSP (Wang et al., 2020) and SynFlow (Tanaka et al., 2020); during training (Zhang et al., 2018; He et al., 2017); and post training (Han et al., 2015a) for different trade-off between training cost and pruned models' quality. (ii) *dynamic sparse training*. It updates model parameters and sparse connectivities at the same time, starting from a randomly sparsified subnetwork (Molchanov et al., 2017). During the training, the removed elements have chances to be grown back if they potentially benefit to predictions. Among the huge family of sparse training (Mocanu et al., 2016; Evci et al., 2019; Mostafa & Wang, 2019; Liu et al., 2021a; Dettmers & Zettlemoyer, 2019; Jayakumar et al., 2021; Raihan & Aamodt, 2020), the recent methods Evci et al. (2020a); Liu et al. (2021b) lead to the state-of-the-art performance.

A special case of static pruning, Lottery tickets hypothesis (LTH) (Frankle & Carbin, 2019), demonstrates the existence of sparse subnetworks in DNNs, which are capable of training in isolation and reach comparable performance of their dense counterpart. The LTH indicates the great potential to train a sparse network from scratch without scarifying expressiveness and has recently drawn lots of attention from diverse fields (Chen et al., 2020b;c;a; Yu et al., 2019; Chen et al., 2021d;b) beyond image recognition (Zhang et al., 2021c; Frankle et al., 2020; Renda et al., 2020).

3 METHODOLOGY

3.1 PRELIMINARIES

Adversarial training (AT). As one of the widely adopted defense mechanisms, adversarial training (Madry et al., 2018b) effectively tackles the vulnerability to maliciously crafted adversarial samples. As formulated in Equation 1, AT (specifically PGD-AT) replaces the original empirical risk minimization into a min-max optimization problem:

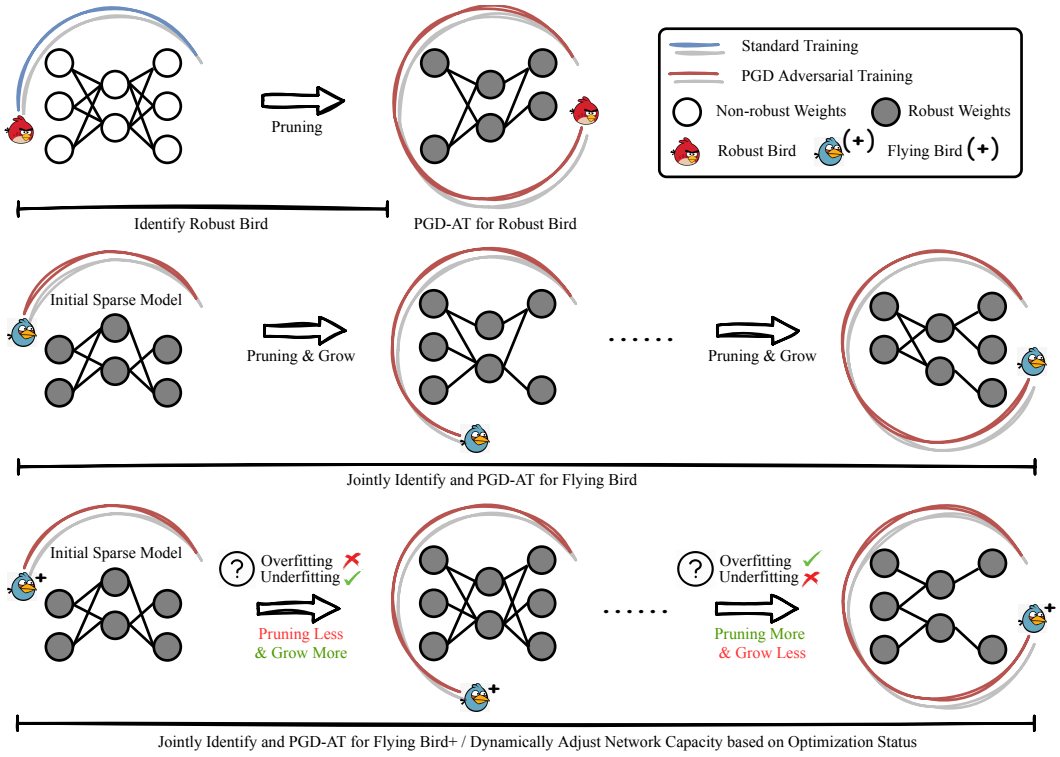

Figure 2: Overview of our proposed training frameworks including Robust Bird (RB), Flying Bird (FB), and Flying Bird (FB+). The length of cycles roughly indicates the number of training epochs.

$$\min_{\theta} \mathbb{E}_{(x,y)\in\mathcal{D}} \mathcal{L}\big(f(x;\theta), y\big) \Longrightarrow \min_{\theta} \mathbb{E}_{(x,y)\in\mathcal{D}} \max_{\|\delta\|_p \leq \epsilon} \mathcal{L}\big(f(x+\delta;\theta), y\big), \tag{1}$$

where $f(x;\theta)$ is a network with parameters θ. Input data x and its associated label y from training set $\mathcal{D}$ are used to first generate adversarial perturbations δ and then minimize the empirical classification loss $\mathcal{L}$. To meet the imperceptible requirement, the ℓ_p norm of δ is constrained by a small constant ϵ. Projected Gradient Descent (PGD), i.e., $\delta^{t+1} = \text{proj}_{\mathcal{P}}[\delta^t + \alpha \cdot \text{sgn}\big(\nabla_x \mathcal{L}(f(x+\delta^t;\theta), y)\big)]$, is usually utilized to produce the adversarial perturbations with step size α, which works in an iterative manner leveraging the local first order information about the network (Madry et al., 2018b).

Sparse subnetworks. Following the routine notations in Frankle & Carbin (2019), $f(x; m \odot \theta)$ donates a sparse subnetwork with a binary pruning mask $m \in \{0,1\}^{\|\theta\|_0}$, where $\odot$ is the element-wise product. Intuitively, it is a copy of dense network $f(x;\theta)$ with a portion of fixed *zero* weights.

3.2 Robust Bird for Adversarial Training

Introducing Robust Bird. The primary goal of *Robust Bird* is to find a high-quality sparse subnetwork efficiently. As shown in Figure 2, it locates subnetworks *quickly* by detecting critical network structures arisen in the early training, which later can be robustified with much less computation.

Specifically, for each epoch t during training, *Robust Bird* creates a sparsity mask m_t by "masking out" the $p\%$ lowest-magnitude weights; then, *Robust Bird* tracks the corresponding mask dynamics. The **key observation** behind *Robust Bird* is that the sparsity mask m_t does *not* change drastically beyond the early epochs of training (You et al., 2020) because high-level network connectivity patterns are learned during the initial stages (Achille et al., 2019). This indicates that *(i)* winning tickets emerge at a very early training stage, and *(ii)* that they can be identified efficiently.

Robust Bird exploits this observation by comparing the Hamming distance between sparsity masks found in consecutive epochs. For each epoch, the last l sparsity masks are stored. If all the stored masks are sufficiently close to each other, then the sparsity masks are not changing drastically over time and network connectivity patterns have emerged; thus, a *Robust Bird* ticket (RB ticket) is drawn. A detailed algorithmic implementation is provided in Algorithm 1 of Appendix A1. This is the RB ticket used in the second stage of adversarial training.

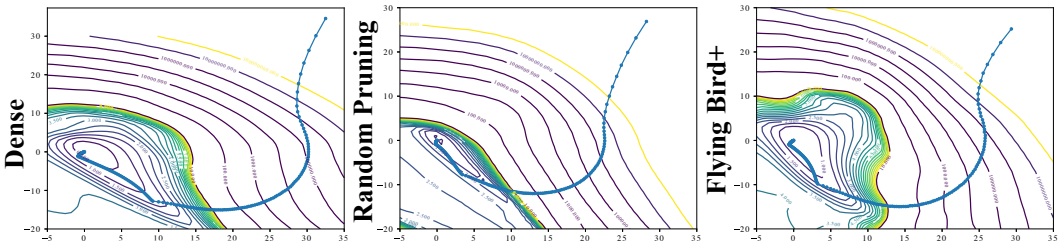

Figure 3: Visualization of loss contours and training trajectories. We compare the dense network, randomly pruned sparse networks, and *flying bird+* at 90% sparsity from ResNet-18 robustified on CIFAR-10.

Rationale of Robust Bird. Recent studies (Zhang et al., 2021b) present theoretical analyses that identified sparse winning tickets enlarge the convex region near the good local minima, leading to improved generalization. Our work also shows a related investigation in Figure A10 that, compared with dense models and random pruned subnetworks, RB tickets found by the standard training have much flatter loss landscapes, serving a high-quality **starting point** for further robustification. This occurs because *flatness* of the loss surface is often believed to indicate the standard generalization. Similarly, as advocated by Wu et al. (2020a); Hein & Andriushchenko (2017), a flatter adversarial loss landscape also effectively shrinks the robustness generalization gap. This "flatness preference" of adversarial robustness has been revealed by numerous empirical defense mechanisms, including Hessian/curvature-based regularization (Moosavi-Dezfooli et al., 2019), learned weight and logits smoothening (Chen et al., 2021c), gradient magnitude penalty (Wang & Zhang, 2019), smoothening with random noise (Liu et al., 2018), or entropy regularization (Jagatap et al., 2020).

These observations make the main cornerstone for our proposal and provide possible interpretations to the surprising finding that the RB tickets pruned from a *non-robust* model can be used for obtaining well-generalizable robust models in the followed robustification. Furthermore, unlike previous costly flatness regularizers (Moosavi-Dezfooli et al., 2019), our methods not only offer a flatter starting point, but also obtain substantial computational savings due to the reduced model size.

3.3 Flying Bird for Adversarial Training

Introducing Flying Bird(+). Since sparse subnetworks from static pruning are unable to regret about removed elements, they maybe too aggressive to capture the pivotal structural patterns. Thus, we introduce *Flying Bird* (FB) to conduct a thorough exploration of dynamic sparsity, which allows pruned parameters to be grown back and engages in the next round of training or pruning, as demonstrated in Figure 2. Specifically, it starts from a sparse subnetwork $f(x; m \odot \theta)$ with a random binary mask m, and then jointly optimize model parameters and sparse connectivities simultaneously. In other words, the subnetwork's typologies are "on the fly", decided dynamically based on current training status. Specifically, we update *Flying Bird*'s sparse connectivity every Δt epochs of adversarial training, which consists of two continually applied operations: pruning and growing. For the pruning step, $p\%$ of model weights with the lowest magnitude will be eliminated, while $g\%$ weights with the largest gradient will be added back in the growth step. Note that newly added connections are not activated in the last sparse topology, and are initialized to zero since it establishes better performance as indicated in (Evci et al., 2020a; Liu et al., 2021b). *Flying Bird* maintains the sparsity ratio unchanged during the full training by keeping both pruning and growing ratio $p\%, g\%$ equal $k\%$ that decays with a cosine annealing schedule.

We further propose *Flying Bird+*, an enhanced variant of FB, capable of adaptively adjusting the sparsity and learning the right parameterization level "on demand" during training, as shown in Figure 2. To be specific, we <u>first</u> record the robust generalization gap and robust validation loss at each training epoch. An increasing generalization gap of the latter training stage indicates a risk of overfitting, while a plateau validation loss implies underfitting. Hence, we <u>then</u> analyse the fitting status according to the upward/downward trend of those measurements. If most epochs (e.g., more than 3 out of the past 5 epochs in our case) tend to see enlarged robust generalization gaps, we raise the pruning ratio $p\%$ to further trim down the network capacity. Similarly, if the majority of epochs present unchanged validation loss, we will increase the growing ratio $q\%$ to enrich the subnetwork capacity. Detailed procedures are summarized in Algorithm 2 of Appendix A1.

Rationale of Flying Bird(+). As demonstrated in Evci et al. (2020a), allowing new connections to grow yields improved flexibility in navigating the loss surfaces, which creates the opportunity to

escape bad local minima and search for the optimal sparse connectivity Liu et al. (2021b). *Flying Bird* follows a similar design philosophy that excludes least important connections (Han et al., 2015a), while activating new connections with the highest potential to decrease the training loss fastest. Recent works (Wu et al., 2020c; Liu et al., 2019) have also found enabling network (re-)growth can turn a poor local minima into a saddle point that facilitates further loss decrease. *Flying Bird+* empowers the flexibility further by adaptive sparsity level control.

The flatness of loss geometry provides another view to dissect the robust generalization gain (Chen et al., 2021c; Stutz et al., 2021; Singla et al., 2021). Figure 3 compares the loss landscapes and training trajectories of dense, randomly pruned subnetworks, and Flying Brid+ robustified on CIFAR-10. We observe that *Flying Bird+* converges to a wider loss valley with improved flatness, which usually suggests superior robust generalization (Wu et al., 2020a; Hein & Andriushchenko, 2017). Last but not the least, our approaches also significantly trim down both the training memory overhead and the computational complexity, enjoying extra bonus of efficient training and inference.

4 Experiment Results

Datasets and architectures. Our experiments consider two popular architectures, ResNet-18 (He et al., 2016), VGG-16 (Simonyan & Zisserman, 2014) on three representative datasets, CIFAR-10, CIFAR-100 (Krizhevsky & Hinton, 2009) and Tiny-ImageNet (Deng et al., 2009). We randomly split one-tenth of the training samples as the validation dataset, and the performance is reported on the official testing dataset.

Training and evaluation details. We implement our experiments with the original PGD-based adversarial trainig (Madry et al., 2018b), in which we train the network against ℓ_∞ adversary with maximum perturbations ϵ of $8/255$. 10-steps PGD for training and 20-steps PGD for evaluation are chosen with a step size α of $2/255$, following Madry et al. (2018b); Chen et al. (2021c). In addition, we also use Auto-Attack (Croce & Hein, 2020) and CW Attack (Carlini & Wagner, 2017) for a more rigorous evaluation. More details are provided in the Appendix A2. For each experiment, we train the network for 200 epochs with an SGD optimizer, whose momentum and weight decay are kept to 0.9 and 5×10^{-4}, respectively. The learning rate starts from 0.1 that decays by 10 times at 100,150 epoch and the batch size is 128, which follows Rice et al. (2020).

For *Robust Bird*, the threshold τ of mask distance is set as 0.1. In *Flying Birds*(+), we calculate the layer-wise sparsity by Ideal Gas Quotas (IGQ) (Vysogorets & Kempe, 2021) and then apply random pruning to initialize the sparse masks. FB updates the sparse connectivity per 2000 iterations of AT, with a update ratio k that starts from 50% and decays by cosine annealing. More details are referred to Appendix A2. Hyperparameters are either tuned by grid search or following Liu et al. (2021b).

Evaluation metrics. In general, we care about both the accuracy and efficiency of obtained sparse networks. To assess the accuracy, we consider both Robust Testing Accuracy (**RA**) and Standard Testing Accuracy (**SA**) which are computed on the perturbed and the original test sets, together with Robust Generalization Gap (**RGG**) (i.e., the gap of RA between train and test sets). Meantime, we report the floating point operations (**FLOPs)** of the whole training process and single image inference to measure the efficiency.

4.1 Robust Bird is a Good Bird

In this section, we evaluate the effectiveness of static sparsity from diverse representative pruning approaches, including: (i) *Random Pruning* (RP), by randomly eliminating model parameters to the desired sparsity; (ii) *One-shot Magnitude Pruning* (OMP), which globally removes a certain ratio of lowest-magnitude weights; (iii) *Pruning at Initialization* algorithms. Three advanced methods, i.e., SNIP (Lee et al., 2019), GraSP (Wang et al., 2020) and SynFlow (Tanaka et al., 2020), are considered, which identify the subnetworks at initialization respect to certain criterion of gradient flow. (iv) *Ideal Gas Quotas* (IGS) (Vysogorets & Kempe, 2021). It adopts random pruning based on pre-calculated layer-wise sparsity which draws intuitive analogies from physics. (v) *Robust Bird* (RB), which can be regarded as a early stopped OMP. (vi) *Small Dense*. It is an important sanity check via considering a smaller dense networks with the same parameter counts as the ones of sparse networks. Comprehensive results of these subnetworks at 80% and 90% sparsity are reported in Table 1, where the chosen sparsity follows routine options (Evci et al., 2020a; Liu et al., 2021b).

Table 1: Performance showing the appearance of poor robust generalization/robust overfitting, and the effectiveness of our sparse proposals with various comparisons to other sparsification methods on CFAIR-10 with ResNet-18. The difference between best and final robust accuracy indicates degradation in performance during training. We pick the best checkpoint by the best robust accuracy on the validation set. Bold numbers indicate superior performance, and ↓ displays shrunk robust generalization gap compared to dense models. Note that model picking criterion and the presentation style are consistent for all tables.

Sparsity(%)	Settings	Robust Accuracy			Standard Accuracy			Training	Inference	Robust
		Best	Final	Diff.	Best	Final	Diff.	FLOPs ($\times 10^{17}$)	FLOPs ($\times 10^{9}$)	Generalization
0	Baseline	51.10	43.61	7.49	81.15	83.38	−2.23	772.41	260.07	38.82
80	Small Dense	49.04	44.18	4.86	76.64	80.77	−4.13	69.54	23.41	21.68 ↓ 17.14
	Random Pruning	49.32	43.97	5.35	77.75	81.27	−3.52	154.40	51.99	25.70 ↓ 13.12
	OMP	50.16	45.02	5.14	79.80	82.39	−2.59	966.63	65.39	28.38 ↓ 10.44
	SNIP	50.46	46.44	4.02	80.13	83.20	−3.07	241.85	81.43	25.24 ↓ 13.58
	GraSP	50.16	45.31	4.85	78.38	82.42	−4.04	187.11	63.00	26.28 ↓ 12.54
	SynFlow	51.17	46.91	4.26	79.08	83.19	−4.11	256.09	86.23	24.66 ↓ 14.16
	IGQ	51.12	46.74	4.38	79.73	83.26	−3.53	239.39	80.60	25.41 ↓ 13.41
	Robust Bird	50.18	46.10	4.08	78.46	82.42	−3.96	209.54	64.64	23.37 ↓ 15.45
	Flying Bird	51.62	46.37	5.25	80.55	83.17	−2.62	239.38	80.60	28.90 ↓ 9.92
	Flying Bird+	51.70	47.51	4.19	80.74	83.16	−2.42	120.04	40.42	23.89 ↓ 14.93
90	Small Dense	46.81	45.48	1.33	77.13	78.54	−1.41	24.31	8.19	13.86 ↓ 24.96
	Random Pruning	47.09	44.97	2.12	75.25	78.77	−3.52	77.16	25.98	15.11 ↓ 23.71
	OMP	49.31	46.11	3.20	77.99	81.00	−3.01	877.76	35.47	19.05 ↓ 19.77
	SNIP	49.49	47.85	1.64	77.74	81.92	−4.18	154.35	51.97	16.20 ↓ 22.62
	GraSP	48.56	46.80	1.76	79.02	81.39	−2.37	113.38	38.18	16.80 ↓ 22.02
	SynFlow	50.08	48.02	2.06	81.15	81.56	−0.41	156.74	52.77	14.68 ↓ 24.14
	IGQ	49.74	48.05	1.69	81.06	81.84	−0.78	141.10	47.51	15.95 ↓ 22.87
	Robust Bird	49.09	46.56	2.53	77.96	80.93.	−2.97	133.42	39.01	16.62 ↓ 22.20
	Flying Bird	50.97	48.10	2.87	79.62	82.93	−3.31	141.10	47.51	20.07 ↓ 18.75
	Flying Bird+	50.88	49.27	1.61	79.95	82.65	−2.70	66.67	22.45	15.16 ↓ 23.66

As shown in Table 1, we first observe the occurrence of poor robust generalization with 38.82% RA gap and robust overfitting with 7.49% RA degradation, when training the dense network (Baseline). Fortunately, coincided with our claims, injecting appropriate sparsity effectively tackle the issue. For instance, RB greatly shrinks the RGG by 15.45%/22.20% at 80/90% sparsity, while also mitigates robust overfitting by $2.53\% \sim 4.08\%$. Furthermore, comparing all *static* pruning methods, we find that (1) Small Dense and RP behave the worst, which suggests the identified sparse typologies play important roles rather than reduced network capacity only; (2) RB shows clear advantages to OMP in terms of all measurements, especially for $78.32\% \sim 84.80\%$ training FLOPs savings. It validates our RB proposal that a few epochs of standard training are enough to learn a high-quality sparse structure for further robustification, and thus there is no need to complete the full training in tickets finding stage like traditional OMP. (3) SynFlow and IGQ approaches have the best RA and SA, while RB obtains the superior robust generalization among static pruning approaches.

Finally, we explore the influence of training regimes during the RB ticket finding on CIFAR-100 with ResNet-18. Table A8 demonstrates that RB tickets perform best when found with the cheapest standard training. Specifically, at 90% and 95% sparsity, SGD RB tickets outperform both Fast AT (Wong et al., 2020) and PGD-10 RB tickets with up to 1.27% higher RA and 1.86% narrower RGG. Figure A8 offers a possible explanation for this phenomenon: the SGD training scheme more quickly develops high-level network connections, during the early epochs of training (Achille et al., 2019). As a result, RB Tickets pruned from model trained with SGD achieve the superior quality.

4.2 Flying Bird is a Better Bird

In this section, we discuss the advantages of dynamic sparsity and show that our Flying Bird(+) is a superior bird. Table 1 examines the effectiveness of FB(+) on CIFAR-10 with ResNet-18, and several consistent observations can be drawn: ❶ FB(+) achieve $9.92\% \sim 23.66\%$ RGG reduction, $2.24\% \sim 5.88\%$ decrease for robust overfitting, compared with the dense network. And FB+ at 80% sparsity even pushes the RA 0.60% higher. ❷ Although the smaller dense network shows the leading performance w.r.t improving robust generalization, the robustness has been largely sacrificed, with up to 4.29% RA degradation, suggesting that only reducing models' parameter counts is insufficient to keep satisfactory SA/RA. ❸ FB and FB+ achieve superior performance of RA for both the *best* and *final* checkpoints across all methods, including RB. ❹ Regardless of small dense and random pruning due to their poor robustness, FB+ reaches the most impressive robust generalization (rank #1 or #2) with the least training and inference costs. Precisely, FB+ obtains $84.46\% \sim 91.37\%$ training FLOPs and $84.46\% \sim 93.36\%$ inference FLOPs saving, i.e., *Flying Bird+ is SUPER light-weight*.

Table 2: Performance showing the effectiveness of our proposed approaches across different datasets with ResNet-18. The subnetworks at 80% sparsity are selected here.

Dataset	Settings	Robust Accuracy			Standard Accuracy			Training	Inference	Robust
		Best	Final	Diff.	Best	Final	Diff.	FLOPs ($\times 10^{17}$)	FLOPs ($\times 10^{9}$)	Generalization
CIFAR-10	Baseline	51.10	43.61	7.49	81.15	83.38	−2.23	772.41	260.07	38.82
	Robust Bird	50.18	46.10	4.08	78.46	82.42	−3.96	209.54	64.64	23.37 $\downarrow$ 15.45
	Flying Bird	51.62	46.37	5.25	80.55	83.17	−2.62	239.38	80.60	28.90 $\downarrow$ 9.92
	Flying Bird+	51.70	47.51	4.19	80.74	83.16	−2.42	120.04	40.42	23.89 $\downarrow$ 14.93
CIFAR-100	Baseline	26.93	19.62	7.31	52.03	53.91	−1.88	772.41	260.07	54.56
	Robust Bird	25.54	20.82	4.72	48.79	53.33	−4.54	189.80	58.00	25.46 $\downarrow$ 29.10
	Flying Bird	26.64	22.00	4.64	53.57	55.41	−1.84	237.12	79.84	27.46 $\downarrow$ 27.10
	Flying Bird+	26.66	23.37	3.29	52.29	55.23	−2.94	100.90	33.97	20.12 $\downarrow$ 34.44
Tiny-ImageNet	Baseline	20.84	15.76	5.08	43.57	46.64	−3.07	6179.30	1040.29	36.84
	Robust Bird	19.58	16.45	3.13	43.70	46.30	−2.60	1410.44	215.15	15.22 $\downarrow$ 21.62
	Flying Bird	20.34	19.00	1.34	45.95	46.86	−0.91	1884.01	317.17	14.93 $\downarrow$ 21.91
	Flying Bird+	20.36	19.11	1.25	45.67	46.73	−1.06	1225.80	206.36	13.24 $\downarrow$ 23.60

Table 3: Performance showing the effectiveness of our proposed approaches with other architectures, i.e., VGG-16 on CIFAR-10/100. The subnetworks at 80% sparsity are selected here.

Architecture	Dataset	Settings	Robust Accuracy			Standard Accuracy			FLOPs		Robust
			Best	Final	Diff.	Best	Final	Diff.	Training	Inference	Generalization
VGG-16	CIFAR-10	Baseline	48.33	42.73	5.60	76.84	79.73	−2.89	574.69	193.50	28.00
		Robust Bird	47.69	41.66	6.03	75.32	78.58	−3.26	165.95	51.48	23.57 $\downarrow$ 4.43
		Flying Bird	48.43	44.65	3.78	77.53	79.72	−2.19	173.56	58.44	21.01 $\downarrow$ 6.99
		Flying Bird+	48.25	45.24	3.01	77.48	79.55	−2.07	94.63	31.86	17.75 $\downarrow$ 10.25
VGG-16	CIFAR-100	Baseline	22.76	18.06	4.70	46.11	46.88	−0.77	574.69	193.50	63.18
		Robust Bird	23.46	17.48	5.98	46.33	47.59	−1.26	165.77	51.42	48.19 $\downarrow$ 14.99
		Flying Bird	22.75	17.96	4.79	46.61	47.36	−0.75	172.14	57.96	48.11 $\downarrow$ 15.07
		Flying Bird+	22.92	19.02	3.90	47.01	48.11	−1.10	69.93	23.54	34.63 $\downarrow$ 28.55

Superior performance across datasets and architectures. We further evaluate the performance of FB(+) across various datasets (CIFAR-10, CIFAR-100 and Tiny-ImageNet) and architectures (ResNet-18 and VGG-16). Table 2 and 3 display that both static and dynamic sparsity of our proposals serve effective remedies for improving robust generalization and mitigating robust overfitting, with $4.43\% \sim 15.45\%$, $14.99\% \sim 34.44\%$ and $21.62\% \sim 23.60\%$ RGG reduction across different architectures on CIFAR-10, CIFAR-100 and Tiny-ImageNet, respectively. Moveover, both RB and FB(+) gain significant efficiency, with up to 87.83% training and inference FLOPs savings.

Superior performance across improved attacks. Additionally, we verify both RB and FB(+) under imporved attacks, i.e., Auto-Attack (Croce & Hein, 2020) and CW Attack (Carlini & Wagner, 2017). As shown in Table A7, our approaches shrink the robust generalization gap by up to 30.76% on CIFAR-10/100, and largely mitigate robust overfitting. This piece of evidence shows our proposal's effectiveness sustained across diverse attacks.

Combining FB+ with existing start-of-the-art (SOTA) mitigation. Previous works (Chen et al., 2021c; Zhang et al., 2021a; Wu et al., 2020b) point out that smoothening regularizations (e.g., KD (Hinton et al., 2015) and SWA (Izmailov et al., 2018)) help robust generalization and lead to SOTA robust accuracies. We combine them with our FB+ and collect the robust accuracy on CIFAR-10 with ResNet-18 in Figure 4. The extra robustness gains from FB+ imply that they makes complementary contributions.

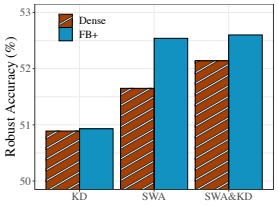

Figure 4: Combination of FB+ and previous SOTAs.

Excluding obfuscated gradients. A common "counterfeit" of robustness improvements is less effective adversarial examples resulted from obfuscated gradients (Athalye et al., 2018). Table A6 demonstrates the maintained enhanced robustness under unseen transfer attacks, which excludes the possibility of gradient masking. More are referred to Section A3.

4.3 Ablation Study and Visualization

Different sparse initialization and update frequency. As two major components in the dynamic sparsity exploration (Evci et al., 2020a), we conduct thorough ablation studies in Table 4 and 5. We found the performance of *Flying Bird+* is more sensitive to different sparse initialization; using SNIP to produce initial layer-wise sparsity and updating the connections per 2000 iterations serves the superior configuration for FB+.

Table 4: Ablation of different sparse initialization in Flying Bird+. Subnetwroks at 80% initial sparsity are chosen on CIFAR-10 with ResNet-18.

Initialization	Robust Accuracy			Standard Accuracy			Robust
	Best	Final	Diff.	Best	Final	Diff.	Generalization
Uniform	49.09	46.96	2.13	78.32	80.32	−2.00	15.61
ERK	50.57	47.70	2.87	79.53	82.21	−2.68	18.64
SNIP	51.30	49.17	2.13	79.86	82.28	−2.42	15.15
GraSP	50.76	47.88	2.88	78.52	82.48	−3.96	18.54
SynFlow	50.56	48.75	1.81	78.51	82.17	−3.66	14.10
IGQ	50.88	49.27	1.61	79.95	82.65	−2.70	15.16

Table 5: Ablation of different update frequency in Flying Bird+. Subnetworks at 80% initial sparsity are chosen on CIFAR-10 with ResNet-18.

Update Frequency	Robust Accuracy			Standard Accuracy			Robust
(iterations)	Best	Final	Diff.	Best	Final	Diff.	Generalization
100	50.32	49.02	1.30	81.28	81.99	−0.71	13.36
500	50.57	48.37	2.20	79.76	82.73	−2.97	18.92
1000	50.99	48.34	2.65	79.55	82.69	−3.14	19.85
2000	51.19	48.39	2.80	79.80	83.00	−3.20	19.17
5000	50.39	48.49	1.90	79.11	82.58	−3.47	17.95
10000	50.08	48.02	2.06	79.25	82.50	−3.25	17.64

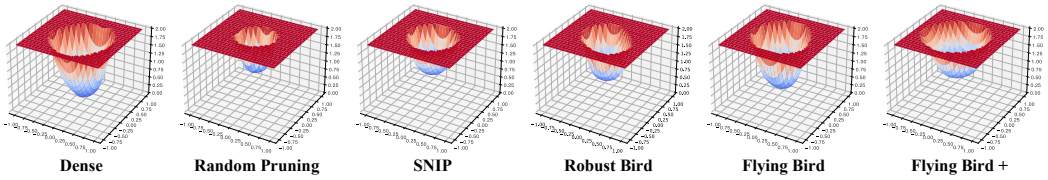

Figure 5: Loss landscape visualization of robusitified dense network and sparse networks (90% sparsity) from different sparsification approaches on CIFAR-10 with ResNet-18.

Final checkpoint loss landscapes. From visualizations in Figure 5, FB and FB+ converge to much more flatter loss valleys, which evidences their effectiveness in closing robust generalization gaps.

Attention and saliency maps. To visually inspect the benefits of our proposal, here we provide attention and saliency maps generated by Grad-GAM (Selvaraju et al., 2017) and tools in (Smilkov et al., 2017). Comparing the dense model to our "talented birds" (e.g., FB+), Figure 6 shows that our approaches have enhanced concentration on main objects, and are capable of capturing more local feature information, aligning better with human perception.

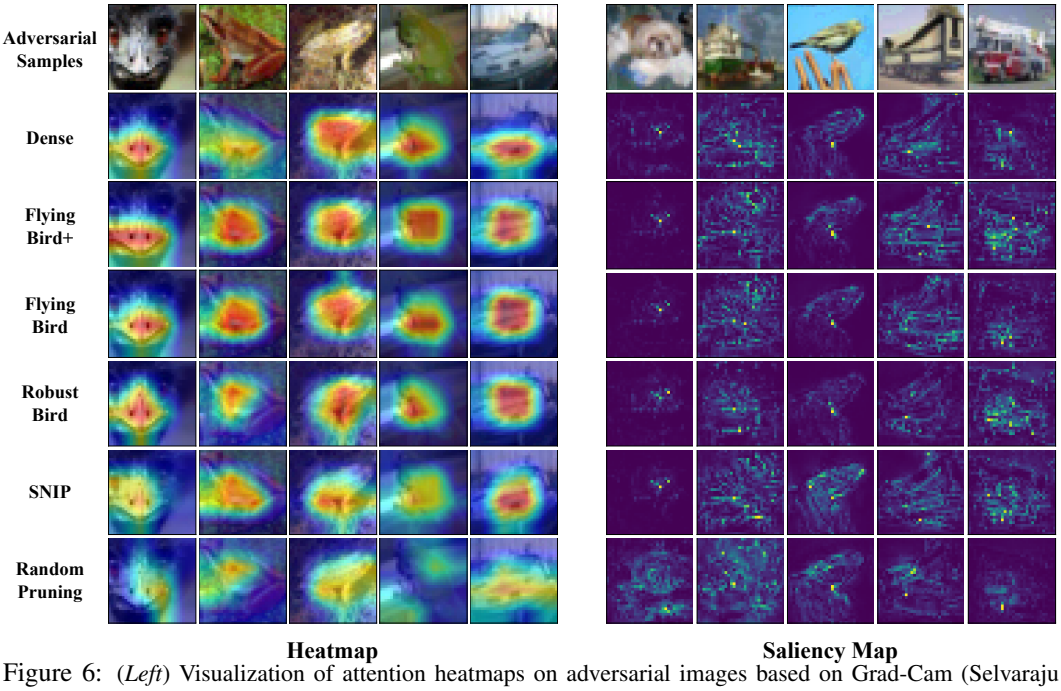

Figure 6: (*Left*) Visualization of attention heatmaps on adversarial images based on Grad-Cam (Selvaraju et al., 2017). (*Right*) Saliency map visualization on adversarial samples (Smilkov et al., 2017).

5 Conclusion

We show the adversarial training of dense DNNs incurs severe robust generalization gap, which can be effectively and efficiently resolved by injecting appropriate sparsity. Our proposed robust birds and flying birds(+) with static and dynamic sparsity, significantly mitigate the robust generalization gap while retain competitive standard/robust accuracy with substantially reduced computation. In the future works, we plan to investigate more sparse structures like channel- and block-wise patterns.

REFERENCES

Alessandro Achille, Matteo Rovere, and Stefano Soatto. Critical learning periods in deep networks. In *International Conference on Learning Representations*, 2019. URL https://openreview.net/forum?id=BkeStsCcKQ.

Anish Athalye, Nicholas Carlini, and David Wagner. Obfuscated gradients give a false sense of security: Circumventing defenses to adversarial examples. *arXiv preprint arXiv:1802.00420*, 2018.

Emilio Rafael Balda, Arash Behboodi, Niklas Koep, and Rudolf Mathar. Adversarial risk bounds for neural networks through sparsity based compression. *arXiv preprint arXiv:1906.00698*, 2019.

Jason Bunk, Srinjoy Chattopadhyay, BS Manjunath, and Shivkumar Chandrasekaran. Adversarially optimized mixup for robust classification. *arXiv preprint arXiv:2103.11589*, 2021.

Nicholas Carlini and David Wagner. Towards evaluating the robustness of neural networks. In *2017 ieee symposium on security and privacy (sp)*, pp. 39–57. IEEE, 2017.

Chen Chen, Jingfeng Zhang, Xilie Xu, Tianlei Hu, Gang Niu, Gang Chen, and Masashi Sugiyama. Guided interpolation for adversarial training. *arXiv preprint arXiv:2102.07327*, 2021a.

Tianlong Chen, Jonathan Frankle, Shiyu Chang, Sijia Liu, Yang Zhang, Michael Carbin, and Zhangyang Wang. The lottery tickets hypothesis for supervised and self-supervised pre-training in computer vision models. *arXiv preprint arXiv:2012.06908*, 2020a.

Tianlong Chen, Jonathan Frankle, Shiyu Chang, Sijia Liu, Yang Zhang, Zhangyang Wang, and Michael Carbin. The lottery ticket hypothesis for pre-trained bert networks. *arXiv*, abs/2007.12223, 2020b.

Tianlong Chen, Jonathan Frankle, Shiyu Chang, Sijia Liu, Yang Zhang, Zhangyang Wang, and Michael Carbin. The lottery ticket hypothesis for pre-trained bert networks. *arXiv preprint arXiv:2007.12223*, 2020c.

Tianlong Chen, Sijia Liu, Shiyu Chang, Yu Cheng, Lisa Amini, and Zhangyang Wang. Adversarial robustness: From self-supervised pre-training to fine-tuning. In *Proceedings of the IEEE/CVF Conference on Computer Vision and Pattern Recognition*, pp. 699–708, 2020d.

Tianlong Chen, Zhenyu Zhang, Sijia Liu, Shiyu Chang, and Zhangyang Wang. Long live the lottery: The existence of winning tickets in lifelong learning. In *International Conference on Learning Representations*, 2021b. URL https://openreview.net/forum?id=LXMSvPmsm0g.

Tianlong Chen, Zhenyu Zhang, Sijia Liu, Shiyu Chang, and Zhangyang Wang. Robust overfitting may be mitigated by properly learned smoothening. In *International Conference on Learning Representations*, 2021c. URL https://openreview.net/forum?id=qZzy5urZw9.

Xuxi Chen, Zhenyu Zhang, Yongduo Sui, and Tianlong Chen. Gans can play lottery tickets too. In *International Conference on Learning Representations*, 2021d. URL https://openreview.net/forum?id=1AoMhc_9jER.

Francesco Croce and Matthias Hein. Reliable evaluation of adversarial robustness with an ensemble of diverse parameter-free attacks. In *International Conference on Machine Learning*, pp. 2206–2216. PMLR, 2020.

Jia Deng, Wei Dong, Richard Socher, Li-Jia Li, Kai Li, and Li Fei-Fei. Imagenet: A large-scale hierarchical image database. In *2009 IEEE conference on computer vision and pattern recognition*, pp. 248–255. Ieee, 2009.

Tim Dettmers and Luke Zettlemoyer. Sparse networks from scratch: Faster training without losing performance. *arXiv preprint arXiv:1907.04840*, 2019.

Guneet S. Dhillon, Kamyar Azizzadenesheli, Jeremy D. Bernstein, Jean Kossaifi, Aran Khanna, Zachary C. Lipton, and Animashree Anandkumar. Stochastic activation pruning for robust adversarial defense. In *International Conference on Learning Representations*, 2018a. URL https://openreview.net/forum?id=H1uR4GZRZ.

Guneet S Dhillon, Kamyar Azizzadenesheli, Zachary C Lipton, Jeremy Bernstein, Jean Kossaifi, Aran Khanna, and Anima Anandkumar. Stochastic activation pruning for robust adversarial defense. *arXiv preprint arXiv:1803.01442*, 2018b.

Chengyu Dong, Liyuan Liu, and Jingbo Shang. Data profiling for adversarial training: On the ruin of problematic data. *arXiv preprint arXiv:2102.07437*, 2021a.

Yinpeng Dong, Fangzhou Liao, Tianyu Pang, Hang Su, Jun Zhu, Xiaolin Hu, and Jianguo Li. Boosting adversarial attacks with momentum. In *Proceedings of the IEEE Conference on Computer Vision and Pattern Recognition*, 2018.

Yinpeng Dong, Ke Xu, Xiao Yang, Tianyu Pang, Zhijie Deng, Hang Su, and Jun Zhu. Exploring memorization in adversarial training. *arXiv preprint arXiv:2106.01606*, 2021b.

Gintare Karolina Dziugaite, Zoubin Ghahramani, and Daniel M Roy. A study of the effect of jpg compression on adversarial images. *arXiv preprint arXiv:1608.00853*, 2016.

Logan Engstrom, Andrew Ilyas, and Anish Athalye. Evaluating and understanding the robustness of adversarial logit pairing. *arXiv preprint arXiv:1807.10272*, 2018.

Utku Evci, Fabian Pedregosa, Aidan Gomez, and Erich Elsen. The difficulty of training sparse neural networks. *arXiv preprint arXiv:1906.10732*, 2019.

Utku Evci, Trevor Gale, Jacob Menick, Pablo Samuel Castro, and Erich Elsen. Rigging the lottery: Making all tickets winners. In *International Conference on Machine Learning*, pp. 2943–2952. PMLR, 2020a.

Utku Evci, Trevor Gale, Jacob Menick, Pablo Samuel Castro, and Erich Elsen. Rigging the lottery: Making all tickets winners. In Hal Daumé III and Aarti Singh (eds.), *Proceedings of the 37th International Conference on Machine Learning*, volume 119 of *Proceedings of Machine Learning Research*, pp. 2943–2952. PMLR, 13–18 Jul 2020b. URL `http://proceedings.mlr.press/v119/evci20a.html`.

Jonathan Frankle and Michael Carbin. The lottery ticket hypothesis: Finding sparse, trainable neural networks. In *International Conference on Learning Representations*, 2019. URL `https://openreview.net/forum?id=rJl-b3RcF7`.

Jonathan Frankle, Gintare Karolina Dziugaite, Daniel M. Roy, and Michael Carbin. Linear mode connectivity and the lottery ticket hypothesis. In *ICML*, 2020.

Ji Gao, Beilun Wang, Zeming Lin, Weilin Xu, and Yanjun Qi. Deepcloak: Masking deep neural network models for robustness against adversarial samples. *arXiv preprint arXiv:1702.06763*, 2017.

Ian Goodfellow, Jonathon Shlens, and Christian Szegedy. Explaining and harnessing adversarial examples. In *International Conference on Learning Representations*, 2015. URL `http://arxiv.org/abs/1412.6572`.

Shupeng Gui, Haotao N Wang, Haichuan Yang, Chen Yu, Zhangyang Wang, and Ji Liu. Model compression with adversarial robustness: A unified optimization framework. *Advances in Neural Information Processing Systems*, 32:1285–1296, 2019.

Chuan Guo, Mayank Rana, Moustapha Cisse, and Laurens van der Maaten. Countering adversarial images using input transformations. In *International Conference on Learning Representations*, 2018a. URL `https://openreview.net/forum?id=SyJ7ClWCb`.

Yiwen Guo, Chao Zhang, Changshui Zhang, and Yurong Chen. Sparse dnns with improved adversarial robustness. *arXiv preprint arXiv:1810.09619*, 2018b.

Song Han, Huizi Mao, and William J Dally. Deep compression: Compressing deep neural networks with pruning, trained quantization and huffman coding. *arXiv preprint arXiv:1510.00149*, 2015a.

Song Han, Jeff Pool, John Tran, and William Dally. Learning both weights and connections for efficient neural network. In *Advances in neural information processing systems*, pp. 1135–1143, 2015b.

Kaiming He, Xiangyu Zhang, Shaoqing Ren, and Jian Sun. Deep residual learning for image recognition. In *CVPR*, pp. 770–778, 2016.

Yihui He, Xiangyu Zhang, and Jian Sun. Channel pruning for accelerating very deep neural networks. In *Proceedings of the IEEE International Conference on Computer Vision*, pp. 1389–1397, 2017.

Matthias Hein and Maksym Andriushchenko. Formal guarantees on the robustness of a classifier against adversarial manipulation. In *Advances in Neural Information Processing Systems*, pp. 2266–2276, 2017.

Geoffrey Hinton, Oriol Vinyals, and Jeff Dean. Distilling the knowledge in a neural network. *arXiv preprint arXiv:1503.02531*, 2015.

Ting-Kuei Hu, Tianlong Chen, Haotao Wang, and Zhangyang Wang. Triple wins: Boosting accuracy, robustness and efficiency together by enabling input-adaptive inference. In *International Conference on Learning Representations*, 2019.

Pavel Izmailov, Dmitrii Podoprikhin, Timur Garipov, Dmitry Vetrov, and Andrew Gordon Wilson. Averaging weights leads to wider optima and better generalization. *arXiv preprint arXiv:1803.05407*, 2018.

Gauri Jagatap, Animesh Basak Chowdhury, Siddharth Garg, and Chinmay Hegde. Adversarially robust learning via entropic regularization. *arXiv preprint arXiv:2008.12338*, 2020.

Siddhant M Jayakumar, Razvan Pascanu, Jack W Rae, Simon Osindero, and Erich Elsen. Top-kast: Top-k always sparse training. *arXiv preprint arXiv:2106.03517*, 2021.

Ziyu Jiang, Tianlong Chen, Ting Chen, and Zhangyang Wang. Robust pre-training by adversarial contrastive learning. *arXiv preprint arXiv:2010.13337*, 2020.

A. Krizhevsky and G. Hinton. Learning multiple layers of features from tiny images. *Master's thesis, Department of Computer Science, University of Toronto*, 2009.

Alexey Kurakin, Ian Goodfellow, and Samy Bengio. Adversarial examples in the physical world. *arXiv preprint arXiv:1607.02533*, 2016.

Yann LeCun, John S Denker, and Sara A Solla. Optimal brain damage. In *Advances in neural information processing systems*, pp. 598–605, 1990.

Namhoon Lee, Thalaiyasingam Ajanthan, and Philip H. S. Torr. Snip: Single-shot network pruning based on connection sensitivity, 2019.

Saehyung Lee, Hyungyu Lee, and Sungroh Yoon. Adversarial vertex mixup: Toward better adversarially robust generalization. In *Proceedings of the IEEE/CVF Conference on Computer Vision and Pattern Recognition*, pp. 272–281, 2020.

F. Liao, M. Liang, Y. Dong, T. Pang, X. Hu, and J. Zhu. Defense against adversarial attacks using high-level representation guided denoiser. In *2018 IEEE/CVF Conference on Computer Vision and Pattern Recognition*, pp. 1778–1787, 2018.

Qiang Liu, Lemeng Wu, and Dilin Wang. Splitting steepest descent for growing neural architectures. *arXiv preprint arXiv:1910.02366*, 2019.

Shiwei Liu, Decebal Constantin Mocanu, Yulong Pei, and Mykola Pechenizkiy. Selfish sparse rnn training. *arXiv preprint arXiv:2101.09048*, 2021a.

Shiwei Liu, Lu Yin, Decebal Constantin Mocanu, and Mykola Pechenizkiy. Do we actually need dense over-parameterization? in-time over-parameterization in sparse training. *arXiv preprint arXiv:2102.02887*, 2021b.

Xuanqing Liu, Minhao Cheng, Huan Zhang, and Cho-Jui Hsieh. Towards robust neural networks via random self-ensemble. In *Proceedings of the European Conference on Computer Vision (ECCV)*, pp. 369–385, 2018.

Zhuang Liu, Jianguo Li, Zhiqiang Shen, Gao Huang, Shoumeng Yan, and Changshui Zhang. Learning efficient convolutional networks through network slimming. In *Proceedings of the IEEE international conference on computer vision*, pp. 2736–2744, 2017.

Aleksander Madry, Aleksandar Makelov, Ludwig Schmidt, Dimitris Tsipras, and Adrian Vladu. Towards deep learning models resistant to adversarial attacks. *arXiv preprint arXiv:1706.06083*, 2017.

Aleksander Madry, Aleksandar Makelov, Ludwig Schmidt, Dimitris Tsipras, and Adrian Vladu. Towards deep learning models resistant to adversarial attacks. In *International Conference on Learning Representations*, 2018a. URL https://openreview.net/forum?id=rJzIBfZAb.

Aleksander Madry, Aleksandar Makelov, Ludwig Schmidt, Dimitris Tsipras, and Adrian Vladu. Towards deep learning models resistant to adversarial attacks. In *International Conference on Learning Representations*, 2018b. URL https://openreview.net/forum?id=rJzIBfZAb.

Decebal Constantin Mocanu, Elena Mocanu, Phuong H Nguyen, Madeleine Gibescu, and Antonio Liotta. A topological insight into restricted boltzmann machines. *Machine Learning*, 104(2): 243–270, 2016.

Dmitry Molchanov, Arsenii Ashukha, and Dmitry Vetrov. Variational dropout sparsifies deep neural networks. In *International Conference on Machine Learning*, pp. 2498–2507. PMLR, 2017.

Pavlo Molchanov, Arun Mallya, Stephen Tyree, Iuri Frosio, and Jan Kautz. Importance estimation for neural network pruning. In *Proceedings of the IEEE Conference on Computer Vision and Pattern Recognition*, pp. 11264–11272, 2019.

Seyed-Mohsen Moosavi-Dezfooli, Alhussein Fawzi, Jonathan Uesato, and Pascal Frossard. Robustness via curvature regularization, and vice versa. In *Proceedings of the IEEE Conference on Computer Vision and Pattern Recognition*, pp. 9078–9086, 2019.

Marius Mosbach, Maksym Andriushchenko, Thomas Trost, Matthias Hein, and Dietrich Klakow. Logit pairing methods can fool gradient-based attacks. *arXiv preprint arXiv:1810.12042*, 2018.

Hesham Mostafa and Xin Wang. Parameter efficient training of deep convolutional neural networks by dynamic sparse reparameterization. In *International Conference on Machine Learning*, pp. 4646–4655. PMLR, 2019.

Preetum Nakkiran. Adversarial robustness may be at odds with simplicity. *arXiv preprint arXiv:1901.00532*, 2019.

Tianyu Pang, Xiao Yang, Yinpeng Dong, Hang Su, and Jun Zhu. Bag of tricks for adversarial training. In *International Conference on Learning Representations*, 2021. URL https://openreview.net/forum?id=Xb8xvrtB8Ce.

Aditi Raghunathan, Sang Michael Xie, Fanny Yang, John C Duchi, and Percy Liang. Adversarial training can hurt generalization. In *ICMLW*, 2019.

Md Aamir Raihan and Tor M Aamodt. Sparse weight activation training. *arXiv preprint arXiv:2001.01969*, 2020.

Alex Renda, Jonathan Frankle, and Michael Carbin. Comparing rewinding and fine-tuning in neural network pruning. In *International Conference on Learning Representations*, 2020.

Leslie Rice, Eric Wong, and Zico Kolter. Overfitting in adversarially robust deep learning. In Hal Daumé III and Aarti Singh (eds.), *Proceedings of the 37th International Conference on Machine Learning*, volume 119 of *Proceedings of Machine Learning Research*, pp. 8093–8104. PMLR, 13–18 Jul 2020. URL http://proceedings.mlr.press/v119/rice20a.html.

Ludwig Schmidt, Shibani Santurkar, Dimitris Tsipras, Kunal Talwar, and Aleksander Madry. Adversarially robust generalization requires more data. In *NeurIPS*, pp. 5014–5026, 2018.

Vikash Sehwag, Shiqi Wang, Prateek Mittal, and Suman Jana. Towards compact and robust deep neural networks. *arXiv preprint arXiv:1906.06110*, 2019.

Ramprasaath R Selvaraju, Michael Cogswell, Abhishek Das, Ramakrishna Vedantam, Devi Parikh, and Dhruv Batra. Grad-cam: Visual explanations from deep networks via gradient-based localization. In *Proceedings of the IEEE international conference on computer vision*, pp. 618–626, 2017.

Karen Simonyan and Andrew Zisserman. Very deep convolutional networks for large-scale image recognition. *arXiv preprint arXiv:1409.1556*, 2014.

Vasu Singla, Sahil Singla, David Jacobs, and Soheil Feizi. Low curvature activations reduce overfitting in adversarial training. *arXiv preprint arXiv:2102.07861*, 2021.

Daniel Smilkov, Nikhil Thorat, Been Kim, Fernanda Viégas, and Martin Wattenberg. Smoothgrad: removing noise by adding noise. *arXiv preprint arXiv:1706.03825*, 2017.

Chuanbiao Song, Kun He, Jiadong Lin, Liwei Wang, and John E Hopcroft. Robust local features for improving the generalization of adversarial training. *arXiv preprint arXiv:1909.10147*, 2019.

David Stutz, Matthias Hein, and Bernt Schiele. Disentangling adversarial robustness and generalization. In *CVPR*, pp. 6976–6987, 2019.

David Stutz, Matthias Hein, and Bernt Schiele. Relating adversarially robust generalization to flat minima. *arXiv preprint arXiv:2104.04448*, 2021.

Ke Sun, Zhanxing Zhu, and Zhouchen Lin. Towards understanding adversarial examples systematically: Exploring data size, task and model factors. *arXiv preprint arXiv:1902.11019*, 2019.

Jihoon Tack, Sihyun Yu, Jongheon Jeong, Minseon Kim, Sung Ju Hwang, and Jinwoo Shin. Consistency regularization for adversarial robustness. *arXiv preprint arXiv:2103.04623*, 2021.

Hidenori Tanaka, Daniel Kunin, Daniel LK Yamins, and Surya Ganguli. Pruning neural networks without any data by iteratively conserving synaptic flow. *arXiv preprint arXiv:2006.05467*, 2020.

Artem Vysogorets and Julia Kempe. Connectivity matters: Neural network pruning through the lens of effective sparsity. *arXiv preprint arXiv:2107.02306*, 2021.

Chaoqi Wang, Guodong Zhang, and Roger Grosse. Picking winning tickets before training by preserving gradient flow, 2020.

Jianyu Wang and Haichao Zhang. Bilateral adversarial training: Towards fast training of more robust models against adversarial attacks. In *Proceedings of the IEEE International Conference on Computer Vision*, pp. 6629–6638, 2019.

Siyue Wang, Xiao Wang, Shaokai Ye, Pu Zhao, and Xue Lin. Defending dnn adversarial attacks with pruning and logits augmentation. In *2018 IEEE Global Conference on Signal and Information Processing (GlobalSIP)*, pp. 1144–1148. IEEE, 2018.

Eric Wong, Leslie Rice, and J. Zico Kolter. Fast is better than free: Revisiting adversarial training. In *International Conference on Learning Representations*, 2020. URL `https://openreview.net/forum?id=BJx040EFvH`.

Dongxian Wu, Yisen Wang, and Shu-tao Xia. Revisiting loss landscape for adversarial robustness. *arXiv preprint arXiv:2004.05884*, 2020a.

Dongxian Wu, Shu-Tao Xia, and Yisen Wang. Adversarial weight perturbation helps robust generalization. In *NeurIPS*, 2020b.

Lemeng Wu, Mao Ye, Qi Lei, Jason D Lee, and Qiang Liu. Steepest descent neural architecture optimization: Escaping local optimum with signed neural splitting. *arXiv preprint arXiv:2003.10392*, 2020c.

Cihang Xie, Jianyu Wang, Zhishuai Zhang, Zhou Ren, and Alan Yuille. Mitigating adversarial effects through randomization. In *International Conference on Learning Representations*, 2018. URL https://openreview.net/forum?id=Sk9yuql0Z.

Weilin Xu, David Evans, and Yanjun Qi. Feature squeezing: Detecting adversarial examples in deep neural networks. *arXiv preprint arXiv:1704.01155*, 2017.

Dingqing Yang, Amin Ghasemazar, Xiaowei Ren, Maximilian Golub, Guy Lemieux, and Mieszko Lis. Procrustes: a dataflow and accelerator for sparse deep neural network training. In *2020 53rd Annual IEEE/ACM International Symposium on Microarchitecture (MICRO)*, pp. 711–724. IEEE, 2020.

Shaokai Ye, Kaidi Xu, Sijia Liu, Hao Cheng, Jan-Henrik Lambrechts, Huan Zhang, Aojun Zhou, Kaisheng Ma, Yanzhi Wang, and Xue Lin. Adversarial robustness vs. model compression, or both? In *Proceedings of the IEEE/CVF International Conference on Computer Vision*, pp. 111–120, 2019.

Haoran You, Chaojian Li, Pengfei Xu, Yonggan Fu, Yue Wang, Xiaohan Chen, Richard G. Baraniuk, Zhangyang Wang, and Yingyan Lin. Drawing early-bird tickets: Toward more efficient training of deep networks. In *International Conference on Learning Representations*, 2020. URL https://openreview.net/forum?id=BJxsrgStvr.

Haonan Yu, Sergey Edunov, Yuandong Tian, and Ari S Morcos. Playing the lottery with rewards and multiple languages: lottery tickets in rl and nlp. *arXiv preprint arXiv:1906.02768*, 2019.

Hongyang Zhang, Yaodong Yu, Jiantao Jiao, Eric Xing, Laurent El Ghaoui, and Michael Jordan. Theoretically principled trade-off between robustness and accuracy. In *International Conference on Machine Learning*, pp. 7472–7482. PMLR, 2019.

Jingfeng Zhang, Xilie Xu, Bo Han, Tongliang Liu, Gang Niu, Lizhen Cui, and Masashi Sugiyama. Noilin: Do noisy labels always hurt adversarial training? *arXiv preprint arXiv:2105.14676*, 2021a.

Shuai Zhang, Meng Wang, Sijia Liu, Pin-Yu Chen, and Jinjun Xiong. Why lottery ticket wins? a theoretical perspective of sample complexity on sparse neural networks, 2021b. URL https://openreview.net/forum?id=8pz6GXZ3YT.

Tianyun Zhang, Kaiqi Zhang, Shaokai Ye, Jian Tang, Wujie Wen, Xue Lin, Makan Fardad, and Yanzhi Wang. Adam-admm: A unified, systematic framework of structured weight pruning for dnns. *arXiv preprint arXiv:1807.11091*, 2018.

Zhenyu Zhang, Xuxi Chen, Tianlong Chen, and Zhangyang Wang. Efficient lottery ticket finding: Less data is more. In *International Conference on Machine Learning*, pp. 12380–12390. PMLR, 2021c.

Dawei Zhou, Nannan Wang, Xinbo Gao, Bo Han, Jun Yu, Xiaoyu Wang, and Tongliang Liu. Improving white-box robustness of pre-processing defenses via joint adversarial training. *arXiv preprint arXiv:2106.05453*, 2021.

Hao Zhou, Jose M Alvarez, and Fatih Porikli. Less is more: Towards compact cnns. In *European Conference on Computer Vision*, pp. 662–677. Springer, 2016.

Bojia Zi, Shihao Zhao, Xingjun Ma, and Yu-Gang Jiang. Revisiting adversarial robustness distillation: Robust soft labels make student better. *arXiv preprint arXiv:2108.07969*, 2021.

A1 MORE TECHNIQUE DETAILS

Algorithms of robust bird and flying bird(+). Here we present the detailed procedure to identify robust bird and flying bird(+), as summarized in algorithm 1 and 2. Note that for the increasing frequency on Line 10 and 11 in algorithm 2, we compare the measurements stored in the queue between two consequent epochs and calculate the frequency of an increasing.

Algorithm 1: Finding a Robust Bird

Input: $f(x;\theta_0)$ w. initialization θ_0, target sparsity $s\%$, FIFO queue Q with length l, threshold τ
Output: Robust bird $f(x; m_{t^*} \odot \theta_{\mathrm{T}})$

1 **while** $t < t_{\max}$ **do**
2 Update network parameters $\theta_t \leftarrow \theta_{t-1}$ via *standard training*
3 Apply static pruning towards target sparsity $s\%$ and obtain the sparse mask m_t
4 Calculate the Hamming distance $\delta_{\mathrm{H}}(m_t, m_{t-1})$, append result to Q
5 $t \leftarrow t + 1$
6 **if** $\max(Q) < \tau$ **then**
7 $t^* \leftarrow t$
8 Rewind $f(x; m_{t^*} \odot \theta_{t^*}) \rightarrow f(x; m_{t^*} \odot \theta_0)$
9 Training $f(x; m_{t^*} \odot \theta_0)$ via PGD-AT for T epochs
10 **return** $f(x; m_{t^*} \odot \theta_{\mathrm{T}})$
11 **end**
12 **end**

Algorithm 2: Finding a Flying Bird(+)

Input: Initialization parameters θ_0, sparse masks m of sparsity $s\%$, FIFO queue Q_p andQ_g with length l, pruning and growth increasing ratio δ_p and δ_g, update threshold ϵ, optimize interval Δt, parameter update ratio $k\%$, ratio update starting point t_{start}
Output: Flying bird(+) $f(x; m \odot \theta_{\mathrm{T}})$

1 **while** $t < \mathrm{T}$ **do**
2 Update network parameters $\theta_t \leftarrow \theta_{t-1}$ via PGD-AT;
3 `# Record training statistics`
4 Add robust generalization gap between train and validation set to Q_p
5 Add robust validation loss to Q_g
6 `# Update sparse masks` m
7 **if** *(t mod* Δt*)* == 0 **then**
8 `|---Optional for Flying Bird+---|`
9 `# Update pruning and growth ratio` $p\%$, $g\%$
10 **if** $t > t_{\mathrm{start}}$ and increasing frequency of $Q_p \geq \epsilon$: $p = (1 + \delta_p) \times k$ **else** $p = k$
11 **if** $t > t_{\mathrm{start}}$ and increasing frequency of $Q_g \geq \epsilon$: $g = (1 + \delta_g) \times k$ **else** $g = k$
12 `|---Optional for Flying Bird+---|`
13 *Prune* $p\%$ parameters with smallest weight magnitude
14 *Grow* $g\%$ parameters with largest gradient
15 Update sparse mask m accordingly
16 **end**
17 **end**

A2 MORE IMPLEMENTATION DETAILS

A2.1 OTHER COMMON DETAILS

We select two checkpoints during training: *best*, which has the best RA values on the validation set, and *final*, i.e., the last checkpoint. And we report both RA and SA of these two checkpoints on test sets. Apart from robust generalization gap, we also show the extent of robust overfitting numerically by the difference of RA between *best* and *final*. Furthermore, we calculate the FLOPs

at both training and inference stage to evaluate the prices of obtaining and exploiting the subnetworks respectively, in which we approximate the FLOPs of the back-propagation to be twice that of forward propagation (Yang et al., 2020).

A2.2 More Details about Robust Bird

For the experiments of RB tickets finding, we comprehensively study three training regimes: standard training with stochastic gradient descent (SGD), adversarial training with PGD-10 AT (Madry et al., 2018b), and Fast AT (Wong et al., 2020). Following Pang et al. (2021), we train the network with an SGD optimizer of 0.9 momentum and 5×10^{-4} weight decay. We use a batch size of 128. For the experiments of PGD-10 AT, we adopt the ℓ_∞ PGD attack with a maximum perturbation $\epsilon = 8/255$ and a step size $\alpha = 2/255$. And the learning rate starts from 0.1, then decay by ten times at $50, 150$ epoch. As for fast AT, we use a cyclic schedule with a maximum learning rate equals 0.2.

A2.3 More Details about Flying Bird(+)

For the experiments of Flying Bird+, the increasing ratio of pruning and growth δ_p, δ_q is kept default to 0.4% and 0.05%, respectively.

Distributions of adopted sparse initialization. We report the layer-wise sparsity of different initial sparse masks. As shown in Figure A7, we observe that subnetworks generally have better performance when the top layers remains most of the parameters.

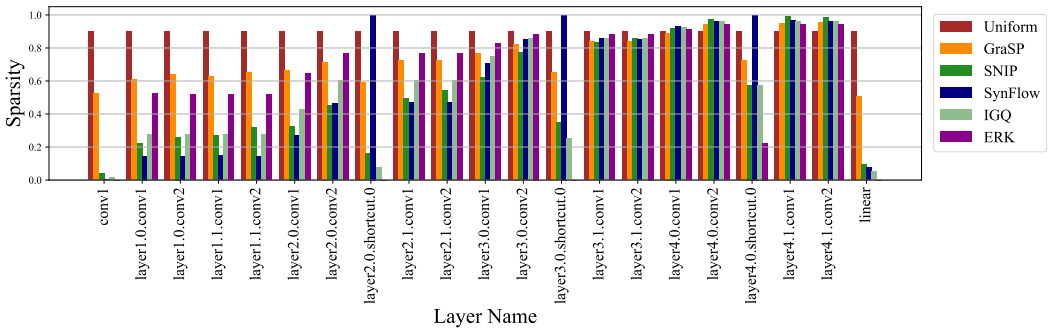

Figure A7: Layer-wise sparisty of different initial sparse masks with ResNet-18

Excluding Obfuscated Gradients. To exclude this possibility of gredient masking, we show that our methods maintain improved robustness under unseen transfer attacks. The left table transfers the attack from an unseen robust model to the above four methods; and the right table shows the transfer testing performance on an unseen robust model (here we use a separately robustified ResNet-50 with PGD-10 on CIFAR-100).

A3 More Experiment Results

A3.1 More Results about Robust Bird

Mask Similarity Visualization. Figure A9 visualizes the dynamic similarity scores for each epoch among masks found via SGD, Fast AT, and PGD-10. Specifically, the similarity scores (You et al., 2020) reflect the Hamming distance between a pair of masks. We notice that masks found by SGD and PGD-10 share more common structures. A possible reason is that Fast AT usually adopts a cyclic learning rate schedule, while SGD and PGD use a multi-step decay schedule.

Different training regimes for finding RB tickets. We denote the subnetworks identified by standard training with SGD, adversarial training with Fast AT (Wong et al., 2020) and adversarial training with PGD-10 AT as SGD tickets, Fast AT tickets and PGD-10 tickets, respectively. Table **??** demonstrate the SGD tickets has the best performance.

Table A6: Transfer attack performance from/on an unseen non-robust model, where the attacks are generated by/applied to the non-robust model. The robust generalization gap is also calculated based on transfer attack accuracies between train and test sets. We use ResNet-18 on CIFAR-10/100 and sub-networks at 80% sparsity.

Dataset	Settings	Transfer Attack from Unseen Model				Transfer Attack on Unseen Model			
		Accuracy			Robust	Accuracy			Robust
		Best	Final	Diff.	Generalization	Best	Final	Diff.	Generalization
CIFAR-10	Baseline	79.68	82.03	−2.35	16.43	70.48	79.85	−9.37	11.84
	Robust Bird	77.33	81.04	−3.71	12.18	73.17	77.03	−3.86	11.49
	Flying Bird	79.13	82.17	−3.04	13.49	71.59	77.19	−5.60	11.88
	Flying Bird+	79.47	81.90	−2.43	11.85	70.43	76.00	−5.57	11.42
CIFAR-100	Baseline	50.51	52.15	−1.64	45.91	48.67	54.48	−5.81	36.98
	Robust Bird	47.25	51.74	−4.49	28.80	47.47	50.90	−3.43	35.82
	Flying Bird	51.80	53.52	−1.72	31.98	45.56	50.61	−5.05	35.39
	Flying Bird+	50.72	53.56	−2.84	25.09	47.04	49.43	−2.39	35.09

Table A7: Evaluation under improved attacks (i.e., Auto-Attack and CW-Attack) on CIFAR-10/100 with ResNet-18 at 80% sparsity. The robust generalization gap is computed under improved attacks.

Dataset	Settings	Auto-Attack				CW-Attack			
		Accuracy			Robust	Accuracy			Robust
		Best	Final	Diff.	Generalization	Best	Final	Diff.	Generalization
CIFAR-10	Baseline	47.41	41.59	5.82	35.30	75.76	66.13	9.63	30.39
	Robust Bird	45.90	42.45	3.45	21.58 ↓ 13.72	73.95	73.52	0.43	17.67 ↓ 12.72
	Flying Bird	47.55	43.57	3.98	26.55 ↓ 8.75	75.30	72.08	3.22	21.77 ↓ 8.62
	Flying Bird+	47.06	44.09	3.17	21.73 ↓ 13.57	76.00	73.83	2.17	17.77 ↓ 12.62
CIFAR-100	Baseline	23.16	17.68	5.48	49.73	45.83	36.21	9.62	57.52
	Robust Bird	21.29	18.00	3.29	21.72 ↓ 28.01	43.30	42.39	0.91	30.82 ↓ 26.70
	Flying Bird	22.74	19.44	3.30	25.18 ↓ 24.55	46.23	42.36	3.87	35.50 ↓ 22.02
	Flying Bird+	22.90	20.31	2.59	19.05 ↓ 30.68	45.86	43.90	1.96	26.76 ↓ 30.76

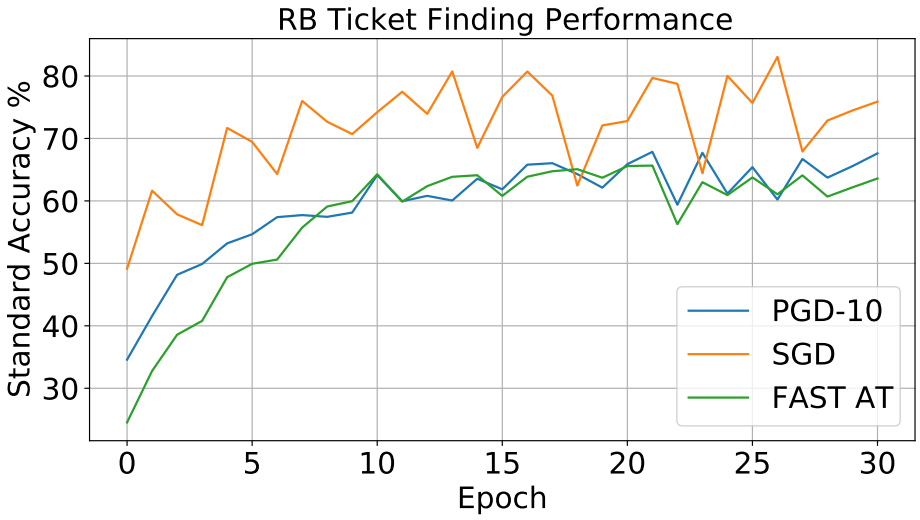

Figure A8: Standard accuracy (SA) of PGD-10, SGD, and Fast AT during the *RB ticket finding* phase.

A3.2 More Results about Flying Bird(+)

We report more results of different sparsification methods across diverse datasets and architectures at Table A9, A10, A11 and A12, from which we observe our approaches are capable of improving robust generalization and mitigating robust overfitting.

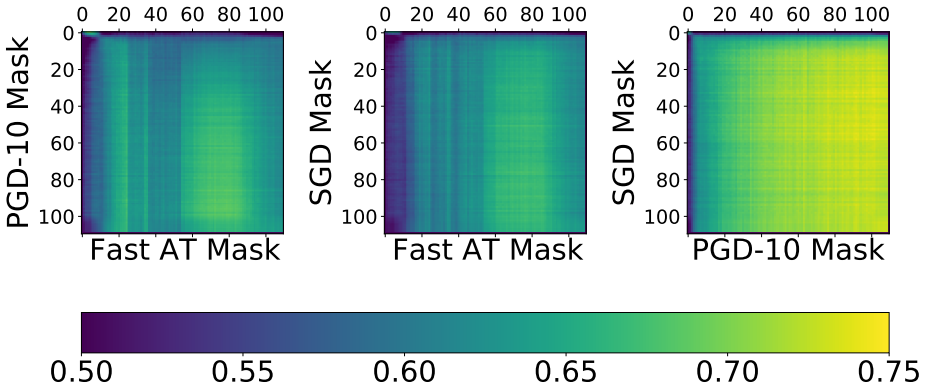

Figure A9: Similarity scores by epoch among masks found via Fast AT, SGD, and PGD-10. A brighter color denotes higher similarity.

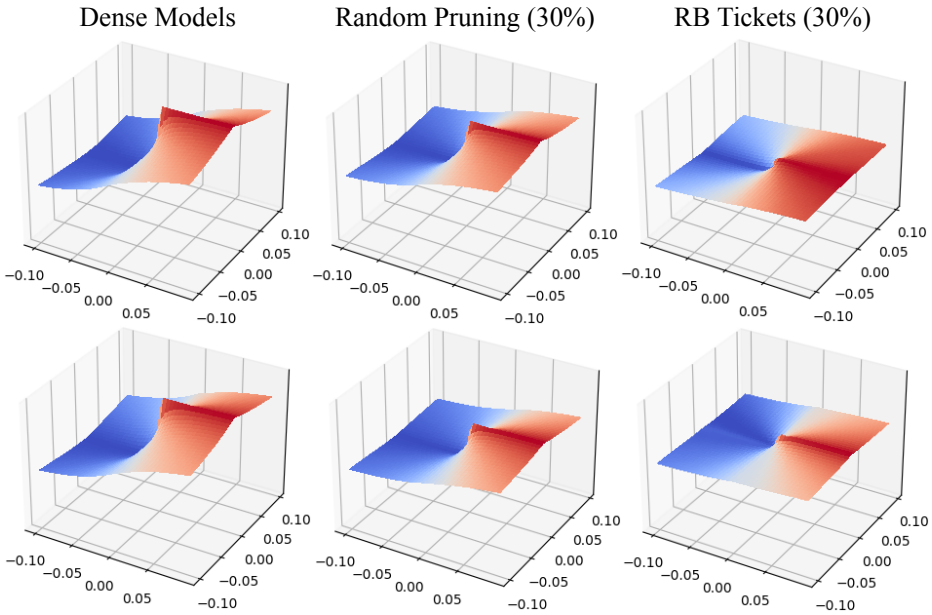

Figure A10: Loss landscapes visualizations Engstrom et al. (2018); Chen et al. (2021c) of the dense model (unpruned), random pruned subnetwork at 30% sparsity, and Robust Bird (RB) tickets at 30% sparsity found by the *standard training*. The ResNet-18 backbone with *the same original initialization* on CIFAR-10 is adopted here. Results demonstrate that RB tickets offer a *smoother* and *flatter* starting point for further robustification in the second stage.

Table A8: Comparison results of different training regimes for RB ticket finding on CIFAR-100 with ResNet-18. The subnetworks at 90% and 95% are selected here.

Sparsity(%)	Settings	Roubst Accuarcy			Standard Accuarcy			Robust
		Best	Final	Diff.	Best	Final	Diff.	Generalization
0	Baseline	26.93	19.62	7.31	52.03	53.91	−1.88	54.56
90	SGD tickets	25.83	23.40	2.43	49.35	53.51	−4.16	18.37 ↓ 36.19
	Fast AT tickets	25.15	22.88	2.27	51.00	51.75	−0.75	20.23 ↓ 34.33
	PGD-10 tickets	25.34	22.96	2.38	52.01	53.27	−1.26	20.03 ↓ 34.53
95	SGD tickets	24.77	24.12	0.65	49.88	50.89	−1.01	9.18 ↓ 45.38
	Fast AT tickets	23.50	22.46	1.04	41.67	43.19	−1.52	9.53 ↓ 45.03
	PGD-10 tickets	24.44	23.77	0.67	49.30	50.65	−1.35	9.86 ↓ 44.70

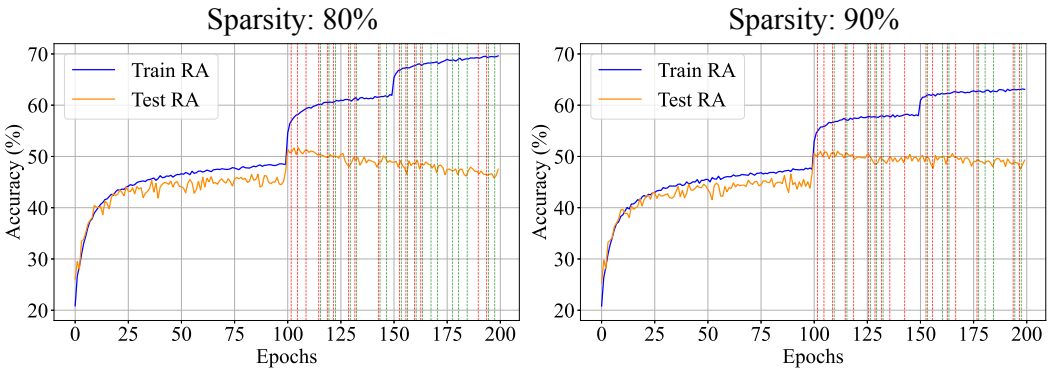

Figure A11: Training curve of Flying Bird+ at 80%(Left) and 90%(Right) sparsity on CIFAR-10 with ResNet-18. The Red and Green dotted lines indicate the time for increasing the pruning and growth ratio, respectively.

Table A9: More results of different sparcification methods on CIFAR-10 with ResNet-18.

Sparsity(%)	Settings	Robust Accuracy			Standard Accuracy			Robust
		Best	Final	Diff.	Best	Final	Diff.	Generalization
0	Baseline	51.10	43.61	7.49	81.15	83.38	−2.23	38.82
95	Small Dense	45.99	44.55	1.44	74.26	75.64	−1.38	7.87 ↓ 30.95
	Random Pruning	45.64	44.18	1.46	75.20	75.20	0.00	7.96 ↓ 30.86
	OMP	47.08	46.23	0.85	78.77	79.36	−0.59	12.01 ↓ 26.81
	SNIP	48.18	46.72	1.46	78.55	79.21	−0.66	9.58 ↓ 29.24
	GraSP	48.58	47.15	1.43	78.95	79.44	−0.49	10.37 ↓ 28.45
	SynFlow	48.93	48.22	0.71	78.70	78.90	−0.20	8.25 ↓ 30.57
	IGQ	48.82	47.56	1.26	79.44	79.76	−0.32	9.33 ↓ 29.49
	Robust Bird	47.53	46.48	1.05	78.33	78.78	−0.45	9.20 ↓ 29.62
	Flying Bird	49.62	48.46	1.16	78.12	81.43	−3.31	13.32 ↓ 25.52
	Flying Bird+	49.37	48.84	0.53	80.33	80.28	0.05	9.27 ↓ 29.55

Table A10: More results of different sparcification methods on CIFAR-10 with VGG-16.

Sparsity(%)	Settings	Robust Accuracy			Standard Accuracy			Robust
		Best	Final	Diff.	Best	Final	Diff.	Generalization
0	Baseline	48.33	42.73	5.60	76.84	79.73	−2.89	28.00
80	Random Pruning	46.14	40.33	5.81	74.42	76.68	−2.26	21.01 ↓ 6.99
	OMP	47.90	43.19	4.71	76.60	80.02	−3.42	24.97 ↓ 3.03
	SNIP	48.03	43.17	4.86	76.68	80.08	−3.40	24.71 ↓ 3.29
	GraSP	47.91	42.34	5.57	75.74	78.87	−3.13	23.65 ↓ 4.35
	SynFlow	48.47	45.32	3.15	77.62	79.09	−1.47	20.17 ↓ 7.83
	IGQ	48.57	44.25	4.32	77.51	80.01	−2.50	22.79 ↓ 5.21
	Robust Bird	47.69	41.66	6.03	75.32	78.58	−3.26	23.57 ↓ 4.43
	Flying Bird	48.43	44.65	3.78	77.53	79.72	−2.19	21.01 ↓ 6.99
	Flying Bird+	48.25	45.24	3.01	77.48	79.55	−2.07	17.75 ↓ 10.25
90	Random Pruning	44.33	40.33	4.00	71.27	74.46	−3.19	15.48 ↓ 12.52
	OMP	47.84	43.34	4.50	75.60	79.10	−3.50	18.29 ↓ 9.71
	SNIP	47.76	44.27	3.49	75.92	79.62	−3.70	17.85 ↓ 10.15
	GraSP	45.96	42.12	3.84	75.19	77.03	−1.84	15.04 ↓ 12.96
	SynFlow	47.54	45.79	1.75	78.43	78.70	−0.27	14.40 ↓ 13.60
	IGQ	47.79	45.12	2.67	74.87	79.19	−4.32	16.06 ↓ 11.94
	Robust Bird	47.09	44.13	2.96	75.53	78.36	−2.83	16.57 ↓ 11.43
	Flying Bird	48.45	45.55	2.90	75.82	79.21	−3.39	16.56 ↓ 11.44
	Flying Bird+	48.39	46.26	2.13	78.73	79.12	−0.39	12.47 ↓ 15.53

Table A11: More results of different sparcification methods on CIFAR-100 with ResNet-18.

Sparsity(%)	Settings	Robust Accuracy			Standard Accuracy			Robust
		Best	Final	Diff.	Best	Final	Diff.	Generalization
0	Baseline	26.93	19.62	7.31	52.03	53.91	−1.88	54.56
80	Small Dense	24.40	21.83	2.57	51.87	51.64	0.23	21.93 ↓ 32.63
	Random Pruning	25.92	20.83	5.09	48.16	51.31	−3.15	34.04 ↓ 20.52
	OMP	25.12	20.18	4.94	50.08	52.81	−2.73	28.57 ↓ 26.00
	SNIP	26.61	23.55	3.06	49.47	54.79	−5.32	23.69 ↓ 30.87
	GraSP	25.37	20.79	4.58	50.27	53.29	−3.02	28.03 ↓ 26.53
	SynFlow	26.31	23.52	2.79	48.33	54.49	−6.16	20.29 ↓ 34.27
	IGQ	26.87	23.07	3.80	49.80	54.39	−4.59	27.04 ↓ 27.52
	Robust Bird	25.54	20.82	4.72	48.79	53.33	−4.54	25.46 ↓ 29.10
	Flying Bird	26.64	22.00	4.64	53.57	55.41	−1.84	27.46 ↓ 27.10
	Flying Bird+	26.66	23.37	3.29	52.29	55.23	−2.94	20.12 ↓ 34.44
90	Small Dense	23.61	22.81	0.80	48.44	48.63	−0.19	11.18 ↓ 43.38
	Random Pruning	24.06	21.45	2.61	47.06	49.73	−2.67	18.04 ↓ 36.52
	OMP	24.45	21.38	3.07	48.02	51.26	−3.24	17.11 ↓ 37.45
	SNIP	26.10	24.46	1.64	52.35	52.88	−0.53	11.54 ↓ 43.02
	GraSP	24.83	22.74	2.09	51.09	52.55	−1.46	14.55 ↓ 40.01
	SynFlow	25.45	24.62	0.83	51.03	51.96	−0.93	10.38 ↓ 44.18
	IGQ	26.22	24.87	1.35	52.37	53.16	−0.79	13.90 ↓ 40.66
	Robust Bird	24.65	22.96	1.69	46.16	51.87	−5.71	16.14 ↓ 38.42
	Flying Bird	26.14	23.57	2.57	50.53	54.78	−4.25	16.73 ↓ 37.83
	Flying Bird+	26.26	24.16	2.10	51.16	53.97	−2.81	11.44 ↓ 43.12

Table A12: More results of different sparcification methods on CIFAR-100 with VGG-16.

Sparsity(%)	Settings	Robust Accuracy			Standard Accuracy			Robust
		Best	Final	Diff.	Best	Final	Diff.	Generalization
0	Baseline	22.76	18.06	4.70	46.11	46.88	−0.77	63.18
80	Random Pruning	22.38	15.76	6.62	41.79	44.85	−3.06	51.15 ↓ 12.03
	OMP	22.98	16.32	6.66	45.45	45.96	−0.51	53.59 ↓ 9.59
	SNIP	23.34	17.83	5.51	46.58	48.55	−1.97	40.42 ↓ 22.76
	GraSP	23.05	16.50	6.55	43.01	46.84	−3.83	49.71 ↓ 13.47
	SynFlow	23.02	17.67	5.35	45.55	47.33	−1.78	41.70 ↓ 21.48
	IGQ	23.60	17.44	6.16	45.77	47.43	−1.66	48.18 ↓ 15.00
	Robust Bird	23.46	17.48	5.98	46.33	47.59	−1.26	48.19 ↓ 15.00
	Flying Bird	22.75	17.96	4.79	46.61	47.36	−0.75	48.11 ↓ 15.07
	Flying Bird+	22.92	19.02	3.90	47.01	48.11	−1.10	34.63 ↓ 28.55
90	Random Pruning	21.48	16.33	5.15	43.10	44.93	−1.83	31.34 ↓ 31.84
	OMP	22.18	17.38	4.80	44.81	45.63	−0.82	38.91 ↓ 24.27
	SNIP	22.92	20.30	2.62	48.50	49.05	−0.55	20.02 ↓ 43.16
	GraSP	22.17	17.60	4.57	44.54	47.00	−2.46	29.76 ↓ 33.42
	SynFlow	22.58	18.88	3.70	43.62	46.73	−3.11	24.96 ↓ 38.22
	IGQ	22.55	18.56	3.99	44.96	48.08	−3.12	27.91 ↓ 35.27
	Robust Bird	22.80	19.19	3.61	45.78	48.61	−2.83	26.46 ↓ 36.72
	Flying Bird	23.59	18.86	4.73	46.64	48.45	−1.81	34.05 ↓ 29.13
	Flying Bird+	23.31	20.34	2.97	45.51	48.13	−2.62	22.16 ↓ 41.02